Journal of Hazardous Materials 515 (2026) 142996

Contents lists available at ScienceDirect

Journal of Hazardous Materials

journal homepage: www.elsevier.com/locate/jhazmat

Source and degradation of plastic debris in the marine environment: A new approach based on carbonyl index and stable isotopes

Pietro Cocozza [a], Eduardo Di Marcantonio [b], Claudia Pelosi [c], Fabrizio Monaci [d,e], Massimo Marchesi [b], Silvia Serranti [a,*]

[a] Department of Chemical Engineering, Materials and Environment, Sapienza University of Rome, Via Eudossiana 18, Rome 00184, Italy
[b] Department of Earth Sciences, Sapienza University of Rome, Rome 00185, Italy
[c] Department of Economics, Engineering, Society and Business Organization, University of Tuscia, Largo dell'Università, Viterbo 01100, Italy
[d] Department of Life Sciences, University of Siena, Via P.A Mattioli 4, Siena 53100, Italy
[e] National Biodiversity Future Center (NBFC), Palermo 90133, Italy

HIGHLIGHTS

- Dual approach combining carbonyl index and stable isotopes for PE pellets.
- Unique comparison of pristine and naturally aged PE pellets from one batch.
- CI increased ~12% after 3 months of marine exposure, indicating oxidation.
- $\delta^{13}C$ remained stable supporting its use as a robust tracer of polymer origin.
- $\delta^{18}O$ positively correlated with CI, indicating photooxidation sensitivity.

GRAPHICAL ABSTRACT

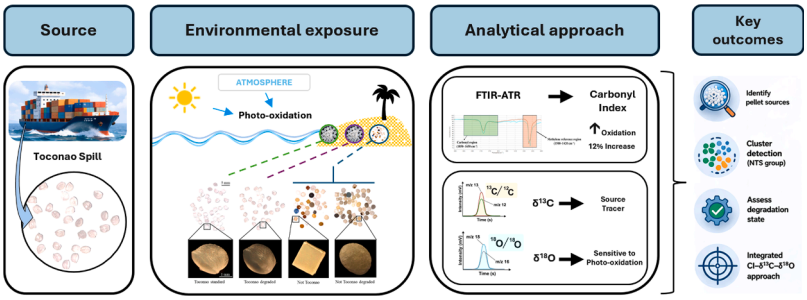

ARTICLE INFO

Keywords:
Plastic pollution
Polyethylene pellets
Carbonyl Index
Stable isotope analysis
Source attribution

ABSTRACT

Plastic pollution in marine environments has become a global concern, emphasizing the need for innovative analytical approaches to trace sources and assess degradation processes. In this study, an integrated analytical approach, combining carbonyl index (CI) and stable isotope analysis ($\delta^{13}C$ and $\delta^{18}O$), was applied to compare polyethylene (PE) pellets retrieved from coastal environments with the corresponding industrial reference material. The study takes advantage of the PE pellet spill from the container ship Toconao, which provided both reference pellets from the original industrial batch and pellets exposed to natural marine conditions for three months, enabling a direct comparison between pristine and environmentally aged material. CI was determined using the SAUB (Specified Area Under Band) method through FTIR-ATR (Fourier Transform InfraRed - Attenuated Total Reflectance) spectroscopy, revealing an average increase of 12.4% after three months of natural exposure, consistent with the formation of new carbonyl groups due to environmental degradation. Carbon isotope analysis showed minimal variation between the standard and exposed samples, indicating preservation of the original isotopic signature during early degradation stages, thus confirming its reliability for tracing plastic sources. In contrast, oxygen isotope analysis report a linkage with CI, highlighting that photooxidative degradation affects the oxygen isotopic composition of the macromolecule, concurrently with the formation of new carbonyl groups. These results demonstrate that the combined spectroscopic-isotopic approach enables

* Corresponding author.
E-mail address: silvia.serranti@uniroma1.it (S. Serranti).

https://doi.org/10.1016/j.jhazmat.2026.142996
Received 21 April 2026; Received in revised form 8 July 2026; Accepted 13 July 2026
Available online 13 July 2026

simultaneous assessment of source and degradation of plastics in the environment, providing a promising tool for large-scale monitoring of plastic origin and aging processes.

1. Introduction

Plastic pollution in marine environments represents one of the most pressing global environmental challenges, with significant impacts on ecosystems, biodiversity and human health [1–6]. Among the various polymers that accumulate in marine and coastal environments, polyethylene (PE) is one of the most abundant and pervasive components [7–14]. Although numerous studies have investigated plastic aging under controlled laboratory conditions, understanding of natural degradation in complex environments, hardly reproducible in the laboratory, remains limited [15–19].

In the perspective of monitoring the residence time and the dispersion of plastic debris, understanding both source and fate is therefore essential. These two dimensions are closely interconnected: assessing the degradation state of a plastic item may constrain its environmental history while identifying its origin can provide information on the initial stage of its dispersion. However, most studies have addressed these questions separately, either focusing on degradation processes or on source apportionment. A comprehensive approach capable of integrating both aspects within a unified analytical framework is still lacking.

With respect to degradation assessment of PE, the Carbonyl Index (CI), measured via FTIR-ATR spectroscopy, has emerged as a valuable proxy [20]. This parameter reflects the accumulation of oxygen-containing functional groups generated during polymer oxidation and is widely used as an indicator of polymer degradation [20,21].

To date, the scientific literature on the study of environmental aging of plastics, with respect to the CI, has predominantly focused on experiments conducted under controlled laboratory conditions, in which plastic degradation is artificially induced through exposure to UV radiation, elevated temperatures, oxidizing chemical agents, or simulated environments, ensuring a direct correspondence with unexposed control samples [19,20]. Its application to field-collected samples, however, remains challenging: the same polymer may undergo heterogeneous degradation depending on exposure conditions, and reference values for “zero-age” materials are rarely available, making it difficult to discriminate between intrinsic production-related variability and true environmental alteration.

In parallel, several approaches have been developed to trace the origin of plastics, including morphological characterization, additive fingerprinting and polymer-specific chemical markers [22,23]. Within this framework, stable isotope analysis, already a widely applied tool for source tracking of chemicals and contaminants [24–29], has recently been proposed for plastic materials. For polymers, the carbon isotopic signature of PE results from both the type and origin of the feedstock and the fractionation processes involved in polymer production. Previous studies have demonstrated the potential of isotopic analysis to differentiate polymer types, distinguish petroleum-based from bio-based plastics and identify plastics from different geographical regions or intended applications [30–33].

In addition, stable isotope analysis can also be used to investigate degradation processes on plastic materials. Recent studies have shown that carbon stable isotopes can be successfully applied to monitor biodegradation processes [30,34]. Although not directly focused on marine-released plastics, Birch et al. (2021) [33] reported that a one-week aging experiment of plastic packaging (not composed of PE) in water under UV exposure did not produce a significant shift in carbon isotopic ratios. In contrast, Berto et al. (2017) [32] observed a shift in carbon isotope composition from PE plastics aged in the Po lagoon (Northern Italy) for 60 days. However, since studies specifically addressing photooxidation remain scarce and the results from literature are not aligned, the carbon isotopic approach may not provide information regarding the photooxidation degradation of the polymer. In fact, since no carbon mass is expected to be lost during photooxidative early stage process, isotopic fractionation should not be significative; photooxidative degradation mainly involves polymer chain scission, likely leaving the initial carbon isotope ratio largely unchanged. In contrast, oxygen isotope ratios could provide more specific insights into degradation processes. External oxygen atoms enter the degraded plastics by binding to the free radicals formed by the breakage [20,21]. In this case, in addition to increasing the percentage composition of oxygen in the pellet, the incoming oxygen could modify the original isotopic composition of the pellet, since it will be mixed with the oxygen already present in the original macromolecule, usually additives [21]. Based on these assumptions, not yet tested in the literature, oxygen stable isotope analysis could be used not only to trace the source of plastics but also to investigate the occurrence and extent of degradation processes.

Within this context, this study proposes and evaluates an integrated analytical framework with three main objectives: i) to test the applicability of the CI as a reliable indicator of in situ degradation when reference material is available, ii) to assess the potential of stable isotope analysis ($\delta^{13}C$ and $\delta^{18}O$) for source attribution and degradation assessment, respectively and iii) to evaluate the complementarity of these methods in view of developing a standardized approach for monitoring plastic source and degradation.

in the environment. To this end, the study takes advantage of a rare field-based sampling condition following the December 2023 plastic pellet spill from the container ship Toconao, in which pristine reference pellets from the original industrial batch were available alongside samples exposed to a well-constrained period of marine exposure of approximately 3 months [14,35]. This unique configuration enables a direct comparison between “time-zero” and environmentally aged materials, overcoming a key limitation of field-based degradation studies.

2. Material and methods

2.1. Plastic pellet sampling and laboratory selection

The samples used in this study were collected as part of the sampling campaign described by Cocozza et al. [14], conducted in March 2024 along the coasts of Galicia and northern Portugal, following the spill of approximately 25,000 kg of plastic pellets from the container ship Toconao (December 8, 2023). Among the collected samples, a subset of pellets from Playa do Rostro, considered the focal area of the beaching event, was selected. At this site, a significant portion of the granules exhibited morphological, chemical, and physical characteristics consistent with those attributed to the pellets released from the Toconao, while other pellets were clearly not related to the spill.

In this study among the pellet samples collected on the beach, only those composed of PE were selected for further analysis. This macrogroup was then subdivided into three distinct categories based on visual and physical characteristics and compared with a group consisting of standard reference pellets. Specifically (Table 1 and Fig. 1):

(1) Toconao Standard (TS): reference PE pellets from the original Toconao batch, characterized by uniform color, weight, shape, and intact surface condition, used as the unexposed time-zero control;
(2) Toconao Degraded (TD): pellets similar to the Toconao standard batch in color, weight and shape, and show minimal signs of environmental degradation;

(3) Not Toconao (NT): pellets that also differ from the Toconao standard in color, weight, and/or shape, but exhibit no visible degradation or only minimal signs of it;
(4) Not Toconao Degraded (NTD): pellets that differ from the Toconao standard in terms of color, weight, and/or shape, and show clear signs of advanced degradation.

The samples were analyzed using the following techniques: FTIR, CI determination and stable isotope analysis ($\delta^{13}C$ and $\delta^{18}O$). The description of sample categories and the number of pellets analyzed for each analytical technique are reported in Table 1. CI and $\delta^{18}O$ analysis were not performed for NT and NTD due to the lack of corresponding pristine reference pellets. Additionally, stable isotope analysis was conducted on a smaller subset of pellets compared to CI, in order to ensure a balanced and representative sampling design while maintaining analytical feasibility. The subset was selected to capture the variability across the defined pellet categories, thereby preserving the representativeness of the isotopic dataset despite the reduced sample size.

Pellets not attributable to the Toconao incident were included in the analysis in order to increase the robustness of the interpretation. Pellets originating from different sources may contain different additives, which can be reflected not only in distinct physical characteristics but also in different spectral profiles [36]. In contrast, the Toconao pellets (TS and TD) are expected to exhibit very similar spectral signatures, providing additional confirmation of their common origin beyond the observed morphological similarities. Furthermore, pellets not attributable to the Toconao (NTD and NT) were considered in the isotopic analysis in order to validate the results obtained by the physical-visual characterization.

2.2. FTIR-ATR spectra acquisition

Plastic samples were analyzed at the Raw Materials Laboratory (RawMaLab) of the Department of Chemical Engineering, Materials and Environment (DICMA), Sapienza University of Rome. Spectral analysis of the pellets was performed using FTIR-ATR in the wavenumber range of 4000–400 cm^{-1}, with an IRAffinity−1S spectrophotometer (Shimadzu Corp., Kyoto, Japan) equipped with a Michelson interferometer (incident angle 30°). Each pellet was analyzed using 40 scans, resulting in a total acquisition time of approximately 40 s per sample. The resulting FT-IR spectra were automatically processed and compared against the polymer database provided by Shimadzu for polymer type identification.

2.3. Carbonyl index

The CI for TD and TS pellet samples was calculated at the Raw Materials Laboratory (RawMaLab) of the Department of Chemical Engineering, Materials and Environment (DICMA), Sapienza University of Rome. The acquired FTIR-ATR spectra were processed using the SAUB method (Specified Area Under Band) [20], to determine the CI. Unlike simpler approaches that rely on the maximum intensity of a spectral peak, the SAUB method integrates the area under specific absorption bands in the IR spectrum, providing a more reliable and reproducible quantification of carbonyl functional groups. The CI, which serves as a quantitative parameter for monitoring the oxidative evolution of polymeric materials, was calculated as the ratio between the area of the carbonyl absorption band (1850–1650 cm^{-1}) and that of the methylene reference band (1500–1420 cm^{-1}), which is commonly used as an internal normalization band due to its relative stability during early stages of polyethylene oxidation.

$$CI = \frac{Area\ under\ band\ 1850 - 1650 \quad cm^{-1}}{Area\ under\ band\ 1500 - 1420 \quad cm^{-1}} \tag{1}$$

.

The CI calculation was performed exclusively on samples belonging to the TS and TD groups, as a comparable analysis involving the NT and NTD groups would have been methodologically invalid due to the absence of a corresponding reference standard for the latter. The lack of a confirmed origin would have compromised the significance of the comparison, introducing uncontrollable variability related to differences in polymer origin and composition. Furthermore, the inner core of five TS and five TD pellets, randomly selected from the overall dataset of 100 TS and 100 TD pellets analyzed for the Cl, was examined to assess the variability between the external surface and the pellet interior.

2.4. Stable isotope analysis

Stable isotope analyses were carried out for carbon and oxygen isotope ratio. The total number of samples prepared for carbon stable isotope analysis (Table 1) was TS = 20, TD = 30, NT = 20, and NTD = 20, whereas for oxygen stable isotope analysis the number of samples was TS = 6 and TD = 20. TS and TD samples were selected after CI analyses to cover the full range of CI variability (low, medium, and high values), including the extremes. The same criterion was applied to the selection of the subset used for inner vs. outer comparisons. For these analyses, approximately 3 mg of material were subsampled from the outer surface of each pellet using a scalpel. However, for $\delta^{1}\,^{3}C$, a random subset of five TS and TD pellets, the inner core of the pellet was also sampled and analyzed.

Carbon isotope measurements were performed at Sapienza LISST (Stable Isotopes Laboratory for Earth Sciences – Department of Earth Sciences) using a Flash Elemental Analyzer (Thermo Fisher Scientific, Bremen, Germany) interfaced in continuous-flow mode with a Delta V Advantage isotope ratio mass spectrometer (Thermo Fisher Scientific, Bremen, Germany). Oxygen stable isotope analyses were conducted at the EASIER facility (National Biodiversity Future Center, University of Siena, Italy) and were obtained using a FlashSmart Elemental Analyzer (EA IsoLink) connected through ConFlo IV to a Delta Q isotope ratio mass spectrometer (Thermo Fisher Scientific, Bremen, Germany). Isotopic ratios were normalized against certified international reference materials (IAEA-CH−6 and IAEA-CH−7 for carbon; IAEA−601, IAEA−600 and USGS−54 for oxygen) and reported in conventional δ-notation (‰) relative to the Vienna Pee Dee Belemnite (V-PDB) standard for carbon and Vienna Standard Mean Ocean Water (V-SMOW) for

Table 1
Description of pellet categories and number of pellets analyzed for each type of analysis: CI, $\delta^{1}\,^{3}C$ and $\delta^{1}\,^{8}O$.

Pellet Category	Origin	Visual degradation	Physical characteristics	FTIR analysis	CI	$\delta^{13}C$	$\delta^{18}O$
Toconao Standard (TS)	Original industrial batch	None	Uniform white coloration, weight and shape	100	100	20	6
Toconao Degraded (TD)	Toconao container ship spill	Minimal	Uniform white coloration, weight and shape	100	100	30	20
Not Toconao (NT)	Industrial/maritime spill-derived pellets	None/minimal	Different color, weight and/or shape	20	/	20	/
Not Toconao Degraded (NTD)	Industrial/maritime spill-derived pellets	Advanced degradation	Different color, weight and/or shape	20	/	20	/

oxygen, according to Eqs. 2 and 3:

$$R = \frac{heavier\ isotope\ abundance}{lighter\ isotope\ abundance} \quad (2)$$

$$\delta \text{ ‰} = \left[\frac{R_{sample}}{R_{standard}} - 1\right] \times 1000 \quad (3)$$

.

2.5. Statistical analysis

All statistical analyses were conducted in R (v4.4.1) using the *stats* package. Descriptive statistics (mean and standard deviation) were calculated for all datasets. For the CI, normality was tested using the Shapiro–Wilk test and differences between TS and TD groups were evaluated using Student's *t*-test and the Wilcoxon signed-rank test. For $\delta^{13}C$, descriptive statistics were calculated and correlations with CI were assessed using Pearson's and Spearman's correlation coefficients. For $\delta^{18}O$, descriptive statistics were calculated and a linear regression was fitted against CI, to visually assess potential relationships, without performing formal statistical inference.

3. Results and discussion

3.1. FTIR-ATR spectra analysis

The analysis conducted on the average FTIR spectra of the four pellet groups (TS, TD, NT, NTD) (Fig. 2) showed a spectral pattern typical of PE. In particular, the characteristic stretching bands of methylene groups (–CH_2–) are evident at approximately ~2915 and ~2848 cm^{-1}, typical of the aliphatic chains of PE. Additional diagnostic signals are observed in the CH_2 bending region at about ~1470–1460 cm^{-1} and in the CH_2 rocking band around 720 cm^{-1}, generally associated with the semicrystalline structure of polyethylene. At the same time, clear spectral differences among the groups were observed in the region between 600 and 1800 cm^{-1}.

The most marked differences emerged between Toconao pellets (TS and TD) and NT/NTD pellets. A clear absorption band at ~1735 cm^{-1} and ~1717 cm^{-1}, attributable to C═O stretching of ester groups, was observed exclusively in the Toconao pellets (TS and TD). This spectral region corresponds to the formation of oxygenated functional groups, typically associated with polymer oxidation processes. However, these groups should be interpreted as the result of a combined effect of additive content and degradation processes, rather than degradation alone, as similarly strong absorption is also observed in TS samples, which are expected to be less affected by environmental degradation. This highlights the importance of reference values when interpreting the CI, which is therefore expected to be significantly different from zero for both TD and TS. Nonetheless, a difference between the TD and TS groups should still be observed, likely reflecting degradation processes. Additional differences were evident in the 1400–1100 cm^{-1} spectral region, associated with C–O–C and C–O stretching vibrations. In particular, the bands at 1350, 1215 and 1159 cm^{-1} show a clear similarity between TS and TD pellets, which consistently display comparable transmittance values and stronger absorption compared to NT and NTD samples. This spectral similarity likely reflects the presence of similar additive formulations within the Toconao pellets. In contrast, such a comparison cannot be meaningfully extended to the NT and NTD groups. In these cases, the averaged spectra were calculated from pellets belonging to different sources and compositions, resulting in greater spectral variability and the absence of a consistent pattern comparable to that observed between TS and TD samples. Overall, the strong spectral similarity between TS and TD pellets across multiple diagnostic bands further supports their common origin and suggests that they likely derive from the same production batch.

3.2. Carbonyl index

The FTIR-ATR analysis conducted on PE pellets from the Toconao spill allowed a sensitive evaluation of the material's oxidative evolution following natural environmental exposure. By applying the SAUB method, the CI was calculated as a parameter to quantify the degree of surface oxidation. The analytical precision of the CI measurements, calculated as the standard deviation of ten samples repeated ten times, was ± 0.01.

The average CI values obtained from each sample (Fig. 3) are 2.58 ± 0.06 for the TS samples and 2.90 ± 0.27 for the TD samples, corresponding to an increase of approximately 12.4% after environmental exposure.

This increase, although moderate, indicates the formation of new carbonyl groups as a result of the interaction between the polymer and environmental factors such as solar radiation, humidity, mechanical action and microbial activity [15,17]. These results demonstrate the sensitivity of the SAUB method in detecting chemical alterations even in the absence of accelerated treatments, such as UV irradiation or

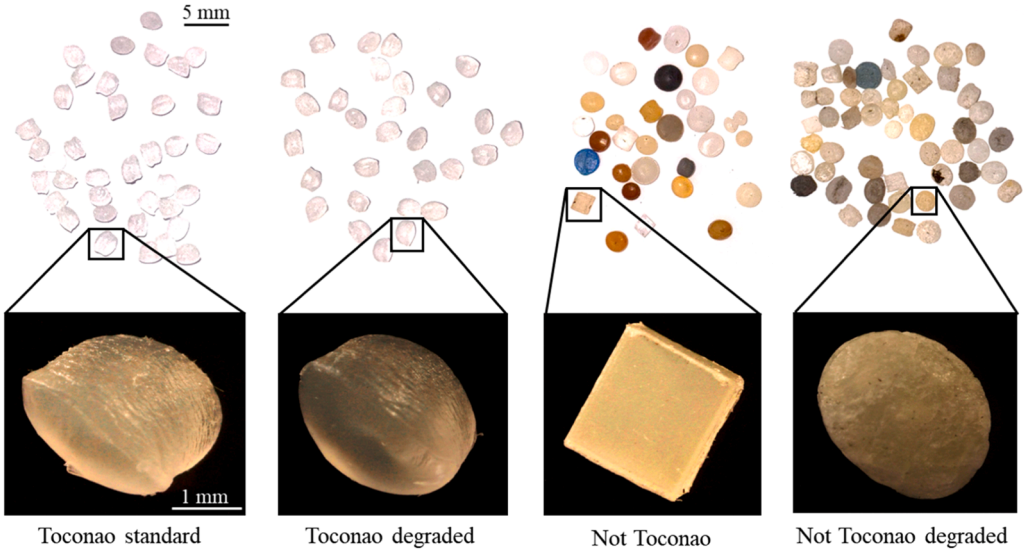

Fig. 1. Example of selected pellets based on the four identified categories.

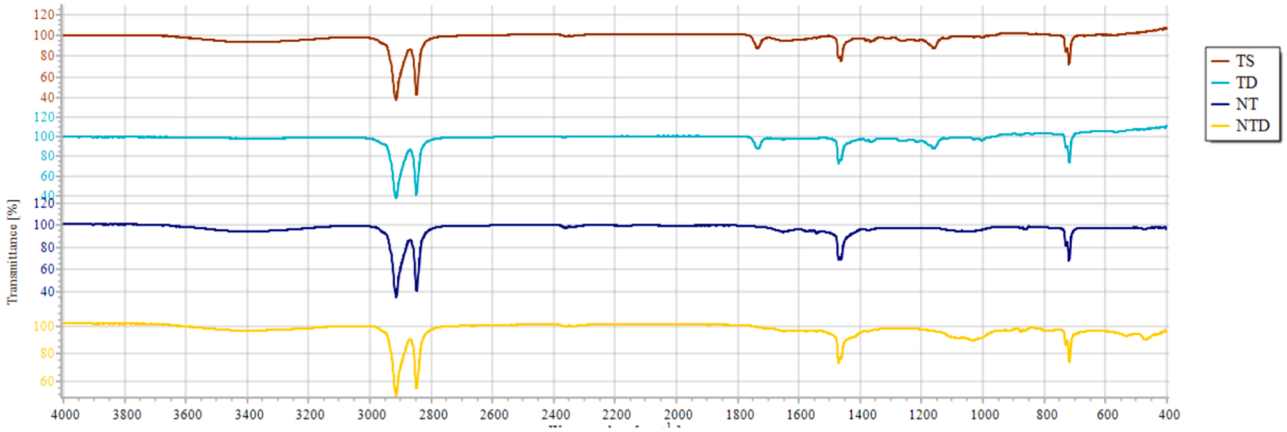

Fig. 2. Average FTIR-ATR spectra of the four pellet groups (TS, TD, NT and NTD). The most evident spectral differences occur in the region between 600 and 1800 cm^{-1}.

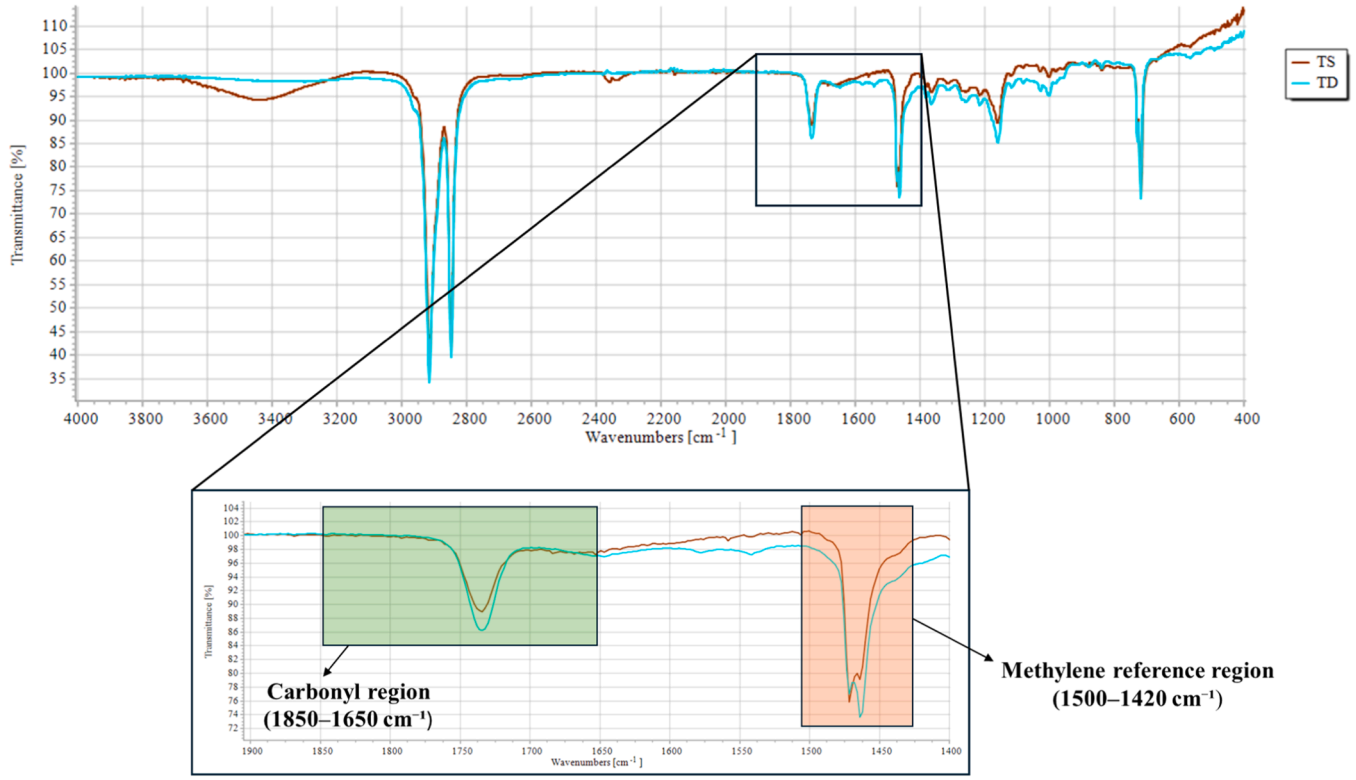

Fig. 3. Comparison between the FTIR-ATR spectra of TS and TD pellets. The highlighted regions correspond to the integration bands used for CI calculation: the carbonyl region (1850–1650 cm^{-1}) and the methylene reference region (1500–1420 cm^{-1}).

exposure to oxidizing agents. Furthermore, it should be noted that the initial CI value measured in the TS samples is relatively high compared with values typically reported for freshly extruded PE materials, which are generally close to zero [20]. This difference may be attributed to the presence of pre-existing carbonyl groups, potentially induced by industrial stabilization processes, storage conditions, presence of additives and processing aids, or handling of the material prior to sampling [37]. Nevertheless, the validity of the comparison between TS and TD samples is not compromised, as both pellet sets originated from the same production batch and underwent the same logistical pathway prior to environmental exposure, ensuring comparable initial conditions.

To the best of our knowledge this study represents the first direct comparison between PE pellets of identical origin subjected to distinct natural conditions (unexposed versus environmentally exposed), without relying on artificial aging protocols. A comparison with existing literature shows that in accelerated photooxidation tests commonly conducted in laboratory settings (e.g., UV exposure at 340 nm for 28 days), CI values for PE pellets increase from approximately 0.03–0.05 to about 0.10–0.14 [21]. The CI value of 2.90 ± 0.27 observed in the TD samples suggests that natural environmental exposure, over a comparable timescale, can result in substantially more pronounced oxidation, compared to the initial value of 2.58 ± 0.06 observed in the TS samples. Similar trends have been reported for PE films exposed directly to marine environments, where increases in carbonyl content were found to be proportional to both the exposure duration and the intensity of physical and biological processes [16]. These observations reinforce the reliability of CI as a diagnostic indicator of oxidative aging in polymers and highlight its potential application to large-scale monitoring of

microplastic degradation programs.

The relatively low standard deviation observed in the TS samples reflects the high homogeneity expected for a non-degraded material originating from the same production batch. The TS mean was taken as the baseline CI at t_0 and subsequently subtracted from TD values. The resulting normalized TD dataset yielded a mean CI of 0.32 ± 0.27, with values spanning from −0.05–1.42.

In contrast, the much higher standard deviation observed in the TD samples indicates considerable heterogeneity in the degree of oxidation among individual pellets.

Inferential statistical testing supported the distinction between TS and TD groups. Shapiro–Wilk tests indicated significant departures from normality for both TS ($p = 7.52 \times 10^{-4}$) and TD ($p = 1.46 \times 10^{-10}$), validating the use of non-parametric comparisons. The Wilcoxon signed-rank test confirmed that CI values differed significantly between groups (statistic = 10000, $p = 2.56 \times 10^{-34}$), while parametric *t*-test results ($t = 82.31$, $df = 108.33$, $p = 1.68 \times 10^{-99}$) corroborated these findings, indicating a strong separation between TS and TD distributions. This observed variability robustly validates the analytical approach adopted so far, confirming its sensitivity in detecting even subtle and heterogeneous environmental impacts on the polymer matrix. Collectively, these results suggest that TD samples underwent measurable alterations in chemical and structural composition, and that such changes can be reliably detected and quantified through CI analysis.

Regarding the analysis of the pellet inner core, the results showed no marked differences between the TS and TD subsets. The CI values measured in the inner portion of the five randomly selected TS and five TD pellets remained comparable and were generally similar to those observed in the TS outer surfaces (Table S1 e S2). In contrast, the outer surfaces of the TD pellets exhibited higher CI values, consistent with the oxidation trends discussed above. This pattern suggests that the oxidative processes associated with environmental exposure were mainly confined to the pellet surface and had not substantially penetrated the polymer bulk. Considering the relatively short environmental exposure period of approximately three months, these findings indicate that degradation was predominantly a surface phenomenon, while the inner core largely retained the chemical characteristics of the original material.

3.3. Stable isotopes

3.3.1. $\delta^{13}C$ as source tracer

The analytical dataset for carbon isotope analysis reported an average cumulative error from standard and sample duplicate of 0.19‰. The mean $\delta^{13}C$ values of the four groups were −28.76‰ for TS, −28.75‰ for TD, −32.06‰ for NT and −29.47‰ for NTD. As shown in Fig. 4, TS displayed very limited variability, with a standard deviation of 0.13‰ and values ranging from −28.92‰ to −28.46‰. In contrast, TD showed a wider spread (st. dev. = 0.26‰; max = −28.11‰; min = −29.33‰), suggesting a greater internal heterogeneity despite having a mean essentially identical to TS. NT and NTD samples, which originated from unknown and heterogeneous sources, exhibited substantially broader variability (NT st. dev. = 1.17‰, range −33.25 to −28.85‰; NTD st. dev. = 3.15‰, range −37.91 to −22.29‰), with extreme outliers particularly evident in NTD group.

The similarity between TS and TD suggests isotopic stability over short environmental residence times, although the lack of independent constraints on exposure duration prevents a quantitative link with degradation. The strong isotopic overlap between TS and TD supports the potential for distinguishing recently dispersed pellets within a limited temporal window (~3 months in this dataset), at a confidence level constrained by TD variability.

Within-group comparisons between TD inner and TD outer, results revealed no significant differences (average shift between TD inner and outer = 0.001‰), indicating spatial homogeneity within the single pellet (Table S2). In contrast, FTIR-derived carbonyl index measurements (Section 3.2) show that chemical alteration is confined to the outer surface, while inner core values are comparable to those of TS samples, confirming that oxidation processes primarily affect the pellet surface. Taken together, these results indicate that photooxidative degradation does not induce measurable changes in bulk $\delta^{1}\,^{3}C$, confirming that it is not measurably affected by this molecular alteration process.

In contrast, NT and NTD (Table S3) differ markedly from TS and TD, indicating that pellets of distinct origin can be isotopically discriminated. Notably, a subgroup of NT samples (NT 7–14) clustered tightly around highly reproducible values (mean = −32.82‰ and st. dev. = 0.02‰), notably different from TS, suggesting that they may derive from a single production source. Therefore, a second visual inspection, in addition to the first one that led to the initial classification of the groups, was carried out (Fig. 5).

A subgroup of NT samples (NT7–14) showed highly consistent $\delta^{1}\,^{3}C$ values (mean = −32.82‰, SD = 0.02‰), clearly distinct from TS, suggesting a common origin. A subsequent re-examination of morphology (Fig. 5) confirmed that these pellets share similar features and indicated that NT1, NT3, and NT5 may also belong to the same group. Based on this combined evidence, these samples were reclassified as a single subgroup (NTS), with an intra-group standard deviation of 0.18‰. FTIR-ATR spectra further support this grouping, showing consistent band patterns indicative of similar polymer composition.

Overall, these results highlight the potential of stable carbon isotopes to support source attribution of environmental plastic pellets, even in the absence of an a priori isotopic reference.

Conversely, the high variability of NTD, consistent with their advanced state of degradation observed visually, precludes firm conclusions but underscores that heavily weathered pellets display large

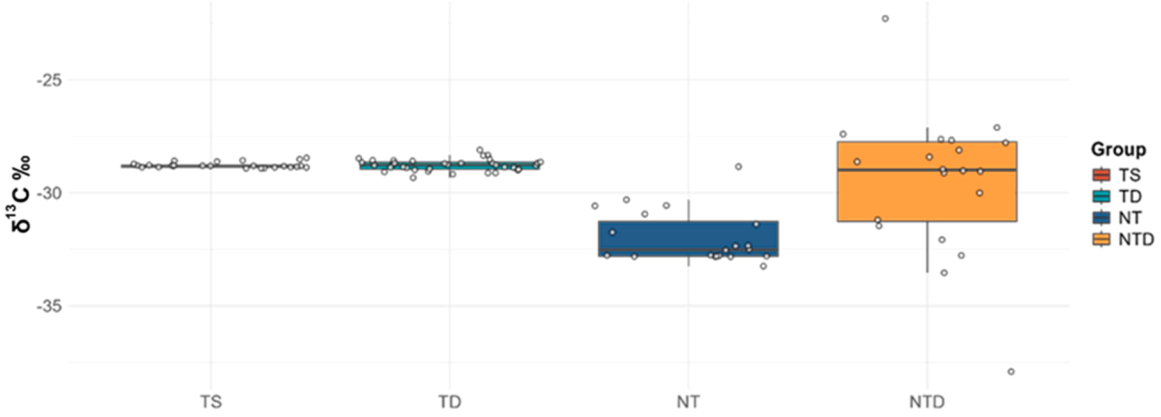

Fig. 4. Boxplots of $\delta^{13}C$ values of the four pellet groups (TS, TD, NT and NTD). Horizontal distribution of the points in the boxplots is random.

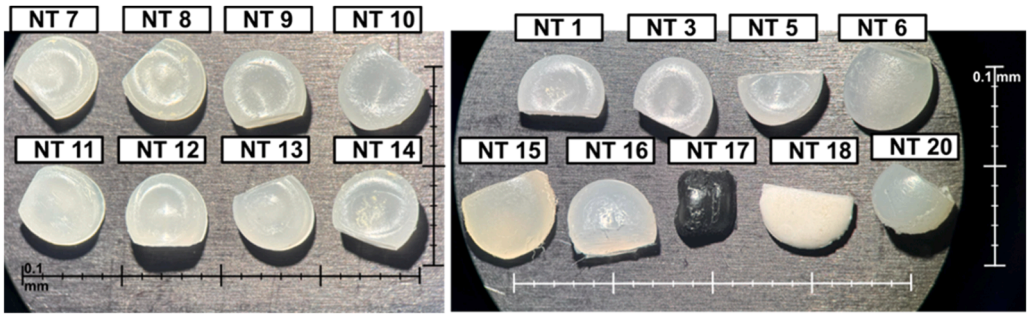

Fig. 5. Stereomicroscope image (×1.25, Leica MZ8) of the NT7−14 group on the left and the other pellets from the NT group on the right. The pellets appear cut because the picture was taken after subsampling for stable isotope analysis. The similarities among pellets NT1, NT3, NT5 and NT7−14 are clearly recognizable in their color, shape, size and the characteristic inward concavity on the surface.

isotopic heterogeneity.

By comparing our results with previous isotopic studies on PE materials, we found that the obtained values are consistent and fall within the same isotopic range. Indeed, PE materials have been reported to exhibit $\delta^{1}\,^{3}C$ values between approximately −32‰ and −27‰ [32,33], which overlaps with the range observed in our dataset for non-degraded pellets (from −33‰ to −28‰).

Although these intervals are broad and largely comparable across studies, this does not exclude the possibility of discriminating specific sources within them. In fact, repeated measurements on standardized material were performed only for the TS group and possibly for the NTS group, providing preliminary evidence that source-level resolution may be achievable.

The absence of a significant carbon isotope ratio shift between TS and TD, despite the measurable increase in carbonyl index, indicates that early oxidative degradation of PE does not measurably affect the carbon isotopic composition of the polymer. This result supports the use of $\delta^{1}\,^{3}C$ as a robust tracer of pellet origin even after environmental exposure.

3.3.2. *Stable isotopes for degradation assessment*

In addition to its successful application for source identification, $\delta^{13}C$ was also tested as a potential tool for assessing the degradation state of pellets, by relating $\delta^{13}C$ values to the CI, which has likewise been successfully employed as an oxidation indicator. Fig. 6 illustrates this dual approach, showing no significant correlation between CI and $\delta^{13}C$ (Pearson r = −0.042, p = 0.824; Spearman ρ = 0.046, p = 0.811).

Based on these results (Fig. 6), no clear isotopic evidence of degradation can be identified for the TD group. As reported by Berto et al. [32], aged plastic debris may exhibit $\delta^{13}C$ enrichments of up to + 2‰ after exposure for as long as 60 days under both experimental and natural conditions. In contrast, no comparable enrichment was observed in the present study, despite evidence of degradation provided by the carbonyl index. Although the shorter residence time of TD pellets may have limited the development of measurable carbon isotope fractionation, additional factors should also be considered. Notably, the degradation process and the molecular alteration are not studied in Berto et al. (2017), making it difficult to determine whether similar degradation pathways were involved. Consequently, processes such as preferential loss of 12C-enriched degradation products, chain scission followed by selective removal of low-molecular-weight compounds, or biodegradation-related fractionation may contribute to $\delta^{13}C$ enrichment under specific conditions. Overall, the present results of our study suggest that, during the early stages of degradation documented here, $\delta^{13}C$ remained largely unaffected by photooxidation and therefore provided limited information on weathering state, while remaining a robust tracer of polymer origin.

Regarding oxygen isotope analyses for degradation assessment, the results showed an error of 0.37‰ and an average value of 12.58‰ and 13.90‰ for TS and TD groups, respectively. The minimum and maximum values observed within the analyzed dataset range between 11.90‰ and 19.00‰. The results of these analyses were not subjected to the same statistical control on correlation with CI (such as Pearson and Spearman test), since the small population size could have produced

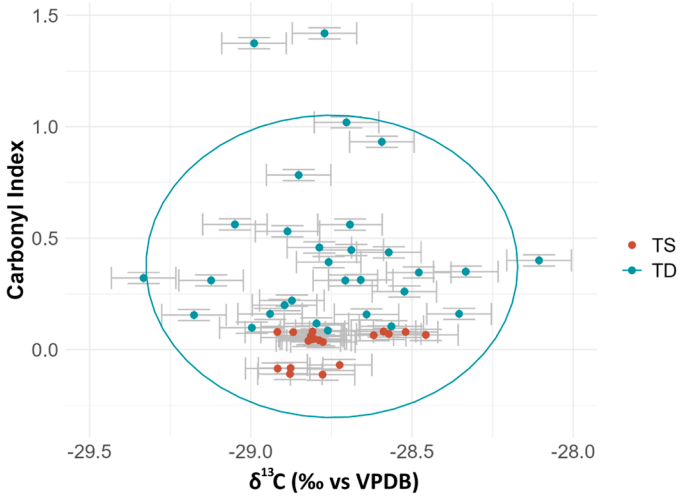

Fig. 6. Scatterplot of $\delta^{13}C$ values versus CI values for TD (light blue) and TS (red) pellets, with associated error bars. The ellipse represents the 95% confidence interval for TD samples. CI values are normalized by subtracting TD samples the mean TS as described in Section 3.2.

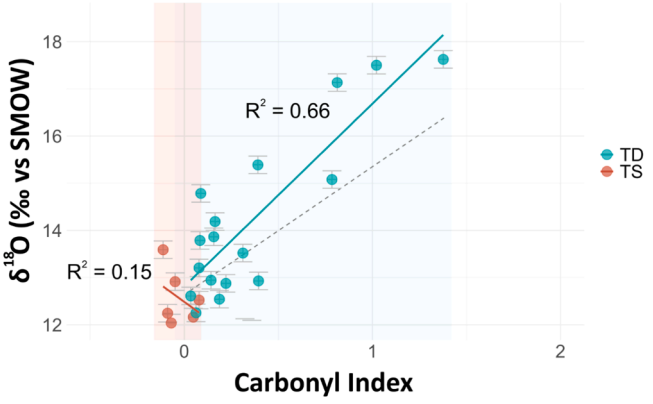

Fig. 7. Scatterplot of CI versus $\delta^{18}O$ for TD (light blue) and TS (red) pellets, with relative error bars. Linear regression lines are shown for each group. The shaded bands represent the CI ranges encompassing all TS data (light red) and all TD data (light blue). The R^2 values for each regression are shown close to the lines. The black dashed line represents the regression line of the calculated point with the isotopic mass balance.

bias. Therefore, the results, showed in Fig. 7, are interpreted using a simple linear regression analysis between CI and $\delta^{18}O$, aiming to a show a possible goodness-of-fit rather than a statistical inference. In general, the scarcity of data limits the strength of the findings, and the conclusions should therefore be interpreted with caution.

Overall, oxygen isotope ratios show greater variability (st.dev. = 1.93) compared to $\delta^{13}C$. Fig. 7 illustrates the relationship between CI and $\delta^{18}O$ for both TD and TS pellets. Furthermore, the TS group shows no significant correlation between $\delta^{18}O$ and CI ($R^2 = 0.15$), and also displays minimal variability in $\delta^{18}O$ (st.dev. = 0.89). In contrast, the TD group exhibits a greater correlation between $\delta^{18}O$ and CI ($R^2 = 0.66$) and higher $\delta^{18}O$ variability (st.dev. = 2.03).

These observations confirm that, for the same range of CI, lower in the TS group, the isotopic signature of oxygen remains constant, likely reflecting the original isotopic composition. Theoretically, PE chain should not contain oxygen atoms; therefore, the initial $\delta^{18}O$ signature and the carbonyl groups already present in the pristine pellets may originate from additives introduced during the manufacturing process, consistent with the relatively high initial CI values discussed in Section 2.1.

The $\delta^{18}O$-CI observed trend in the TD group suggests a positive correlation, highlighting an isotopic enrichment in heavy oxygen isotopes with increasing CI. This trend likely reflects photooxidation processes involving multiple oxygen sources, the most probable of which, given the increasing $\delta^{18}O$ values with increasing carbonyl index (CI), appears to be atmospheric oxygen, characterized by higher $\delta^{18}O$ values (~ 23.5‰) [38,39] than the pristine polymer (12.58‰) In order to evaluate the role of atmospheric oxygen as the primary oxygen source, theoretical $\delta^{18}O$ values were calculated using an isotopic mass balance approach, in which the carbonyl index (CI) was used as quantitative parameter for the extent of oxygen incorporation. The model assumes atmospheric oxygen as the dominant source and is expressed as follows:

$$CI_{TD} \times \delta^{18}O_{TD} = CI_{TS} \times \delta^{18}O_{TS} + (CI_{TD} - CI_{TS}) \times \delta^{18}O_{atmosphere} \quad (4)$$

.

In this formulation, the $\delta^{18}O$ values of the TD and TS groups are weighted by their respective CI values, while the increase in CI between the two groups is associated with the isotopic signature of atmospheric oxygen (~23.5‰). This simplified framework is intended to estimate the expected $\delta^{18}O$ values under the assumption of a single dominant oxygen source and to test the consistency of the proposed interpretation. As shown in Fig. 7, the measured $\delta^{18}O$ values exhibit a steeper regression slope (4.45) compared to the calculated values (2.84), indicating a deviation from the simplified model. Although this discrepancy may partly reflect the limited size of the dataset and does not allow for definitive conclusions, it suggests that the system is not fully described by a single-source incorporation model. Among the possible explanations, the most plausible relates to the limitations of the carbonyl index as a quantitative proxy for total oxygen incorporation. The CI specifically accounts for carbonyl-containing functional groups, whereas photooxidation of polyethylene also produces a broader suite of oxygenated species, including hydroperoxides, alcohols, and carboxylic acids. These additional functional groups are not captured by CI but contribute to the total oxygen pool measured isotopically, potentially leading to an underestimation of the true extent of oxygen incorporation in more degraded samples. This effect becomes increasingly relevant at higher degrees of degradation, where secondary oxidation pathways are more pronounced. In addition, contributions from other oxygen reservoirs, such as dissolved seawater oxygen (typically around 0‰ [40]), cannot be completely excluded, although their involvement alone would not readily explain the observed enrichment pattern. Kinetic isotope effects associated with radical-driven oxidation may further modulate the isotopic distribution between oxygen sources and the polymer matrix.

Taken together, these factors may lead to an underestimation of the total isotopic exchange when relying exclusively on CI-based quantification, particularly in more degraded samples. Overall, while multiple processes and oxygen reservoirs may contribute to isotopic variability, the results of this preliminary analysis are consistent with photooxidation processes primarily driven by incorporation of atmospheric oxygen, with secondary modifications arising from incomplete representation of oxygenated functional groups by the carbonyl index.

However, over the maximum experimental duration under natural exposure conditions (approximately three months), the number of highly degraded samples remains insufficient to support robust conclusions or to develop statistically meaningful degradation models.

Overall, both CI and $\delta^{18}O$ appear to trace different aspects of the same degradation mechanism. However, the limited size of the oxygen isotope dataset prevents the formulation of strong assumptions, and a larger dataset will be required to confirm the observed correlation between CI and $\delta^{18}O$.

4. Conclusions

This study demonstrates the potential of a combined FTIR-ATR carbonyl index (CI) and stable isotope ($\delta^{13}C$ and $\delta^{18}O$) approach to investigate both the origin and environmental alteration of polyethylene pellets in marine environments. CI values, determined using the SAUB method, proved to be a sensitive indicator of early oxidative degradation, with environmentally exposed pellets (TD) showing a 12.4% increase relative to reference samples (TS), consistent with carbonyl formation.

Stable carbon isotope ratios ($\delta^{13}C$) remained effectively invariant after approximately three months of marine exposure (−28.75‰ for TD vs. −28.76‰ for TS), confirming their robustness as tracers of polymer origin and enabling discrimination between Toconao-derived pellets and those of unknown provenance.

Oxygen isotope data ($\delta^{18}O$), although based on a limited dataset, show a preliminary association with CI variability, suggesting a potential link between oxygen incorporation and oxidation processes. However, further data are required to confirm this relationship.

Overall, the combined CI–$\delta^{13}C$–$\delta^{18}O$ framework provides complementary information on polymer source and early-stage degradation, although its current application remains constrained by limited temporal coverage and sample size. To operationalize this approach for addressing plastic pollution, further developments are required, both in the lab and campaign scale. Future work should focus on controlled laboratory aging experiments designed to quantify isotopic and chemical fractionation under well-defined environmental conditions. Moreover, additional sampling campaigns in the same geographical areas will also be necessary to verify the robustness and reproducibility of the proposed protocol under realistic environmental variability, thereby strengthening confidence in its applicability across different spatial and temporal contexts.

In conclusion, the integrated CI-$\delta^{18}O$-$\delta^{13}C$ methodology represents a promising tool for the environmental monitoring of plastics, capable of addressing both source and fate of plastic contaminants in a complementary manner. The proposed developments will be crucial to transform this approach from a proof-of-concept into an operational tool, improving the quantification of microplastic environmental persistence and supporting more effective mitigation strategies.

Environmental implication

This study provides rare field-based evidence of polyethylene pellet degradation under real marine conditions, enabled by the availability of both pristine and environmentally exposed materials from the same production batch, following the *Toconao* spill. The integration of FTIR-derived carbonyl index (CI) and stable isotope analysis ($\delta^{13}C$, $\delta^{18}O$) allows simultaneous assessment of degradation processes and source attribution. While $\delta^{13}C$ remains stable and suitable for tracing origin, CI and $\delta^{18}O$ capture oxidative weathering. This combined approach

improves discrimination between spill-related and background microplastics and offers a robust tool for environmental forensics and large-scale monitoring of plastic pollution.

CRediT authorship contribution statement

Pietro Cocozza: Writing – original draft, Methodology, Investigation, Formal analysis, Data curation, Conceptualization. **Eduardo Di Marcantonio:** Writing – original draft, Methodology, Formal analysis, Data curation, Conceptualization. **Claudia Pelosi:** Writing – review & editing, Supervision, Software. **Fabrizio Monaci:** Writing – review & editing, Resources. **Massimo Marchesi:** Writing – review & editing, Validation, Supervision. **Silvia Serranti:** Writing – review & editing, Validation, Supervision, Resources, Methodology, Conceptualization.

Declaration of Competing Interest

The authors declare that they have no known competing financial interests or personal relationships that could have appeared to influence the work reported in this paper.

Acknowledgements

This work was supported by Sapienza University of Rome through the "Call for funding for periods of mobility abroad for PhD students of the XXXVII and XXXVIII cycles", which enabled the mobility of Dr. Pietro Cocozza to the University of Cadiz. The authors also thank Prof. Giorgio Anfuso (University of Cadiz) for logistical support during the field activities in Spain.

Appendix A. Supporting information

Supplementary data associated with this article can be found in the online version at doi:10.1016/j.jhazmat.2026.142996.

Data availability

Data will be made available on request.

References

[1] Andrady, A.L., 2011. Microplastics in the marine environment. Mar Pollut Bull 62, 1596–1605. https://doi.org/10.1016/j.marpolbul.2011.05.030.
[2] Iannilli, V., Di Gennaro, A., Lecce, F., Sighicelli, M., Falconieri, M., Pietrelli, L., Poeta, G., Battisti, C., 2018. Microplastics in Talitrus saltator (Crustacea, Amphipoda): new evidence of ingestion from natural contexts. Environ Sci Pollut Res 25, 28725–28729. https://doi.org/10.1007/s11356-018-2932-z.
[3] Hoseini, M., Bond, T., 2022. Predicting the global environmental distribution of plastic polymers. Environ Pollut 300. https://doi.org/10.1016/j.envpol.2022.118966.
[4] Tuna, A., Taş, B.M., Başaran Kankılıç, G., Koçak, F.M., Şencan, Z., Cömert, E., Bayar Muluk, N., Kaçmaz, B., Gül, S., Böke, E., 2023. Detection of microplastics in patients with allergic rhinitis. Eur Arch Oto-Rhino-Laryngol 280, 5363–5367. https://doi.org/10.1007/s00405-023-08105-7.
[5] Cocozza, P., Serranti, S., Setini, A., Cucuzza, P., Bonifazi, G., 2024. Monitoring of contamination by microplastics on sandy beaches at Vulcano Island (Sicily, Italy) by hyperspectral imaging. Environ Sci Pollut Res. https://doi.org/10.1007/s11356-024-34972-6.
[6] Welsh, B., Bennett, E., Paterson, A.M., Yao, H., Drouillard, K., Aherne, J., 2026. Beyond the surface: Stratification and turnover control microplastic dynamics in a seasonally ice-covered sentinel lake. J Hazard Mater 502. https://doi.org/10.1016/j.jhazmat.2025.140917.
[7] Karlsson, T.M., Arneborg, L., Broström, G., Almroth, B.C., Gipperth, L., Hassellöv, M., 2018. The unaccountability case of plastic pellet pollution. Mar Pollut Bull 129, 52–60. https://doi.org/10.1016/j.marpolbul.2018.01.041.
[8] Erni-Cassola, G., Zadjelovic, V., Gibson, M.I., Christie-Oleza, J.A., 2019. Distribution of plastic polymer types in the marine environment; A meta-analysis. J Hazard Mater 369, 691–698. https://doi.org/10.1016/j.jhazmat.2019.02.067.
[9] Chen, Y., Li, X., Shu, Y., Li, Z., Yang, G., Wang, J., Wu, Q., Cao, W., Li, E., Liu, Y., Li, W., Lv, G., 2026. PE microplastics altered microbial resource limitation and C/N use efficiency in cotton rhizosphere soil. J Hazard Mater 503. https://doi.org/10.1016/j.jhazmat.2026.141267.
[10] Spalding Mark A, Ananda Chatterjee, Handbook of industrial polyethylene and technology: definitive guide to manufacturing, properties, processing, applications and markets, 2017.
[11] Suaria, G., Avio, C.G., Mineo, A., Lattin, G.L., Magaldi, M.G., Belmonte, G., Moore, C.J., Regoli, F., Aliani, S., 2016. The Mediterranean Plastic Soup: Synthetic polymers in Mediterranean surface waters. Sci Rep 6. https://doi.org/10.1038/srep37551.
[12] Zhang, H., 2017. Transport of microplastics in coastal seas. Estuar Coast Shelf Sci 199, 74–86. https://doi.org/10.1016/j.ecss.2017.09.032.
[13] Zeng, Y., Wang, H., Liang, D., Yuan, W., Li, S., Xu, H., Chen, J., 2024. Navigating the difference of riverine microplastic movement footprint into the sea: Particle properties influence. J Hazard Mater 476. https://doi.org/10.1016/j.jhazmat.2024.134888.
[14] Cocozza, P., Scarrica, V.M., Rizzo, A., Serranti, S., Staiano, A., Bonifazi, G., Anfuso, G., 2025. Microplastic pollution from pellet spillage: Analysis of the Toconao ship accident along the Spanish and Portuguese coasts. Mar Pollut Bull 211. https://doi.org/10.1016/j.marpolbul.2024.117430.
[15] Hakkarainen, M., Albertsson, A.C., 2004. Environmental degradation of polyethylene. Adv Polym Sci 169, 177–199. https://doi.org/10.1007/b13523.
[16] Lourmpas, N., Papanikos, P., Efthimiadou, E.K., Fillipidis, A., Lekkas, D.F., Alexopoulos, N.D., 2024. Degradation assessment of high-density polyethylene (HDPE) debris after long exposure to marine conditions. Sci Total Environ 954, 176847. https://doi.org/10.1016/j.scitotenv.2024.176847.
[17] Gao, R., Sun, C., 2021. A marine bacterial community capable of degrading poly (ethylene terephthalate) and polyethylene. J Hazard Mater 416. https://doi.org/10.1016/j.jhazmat.2021.125928.
[18] Alvarez-Zeferino, J.C., Beltrán-Villavicencio, M., Vázquez-Morillas, A., 2015. Degradation of Plastics in Seawater in Laboratory. Open J Polym Chem 05, 55–62. https://doi.org/10.4236/ojpchem.2015.54007.
[19] Zha, F., Dai, J., Han, Y., Liu, P., Wang, M., Liu, H., Guo, X., 2023. Release of millions of micro(nano)plastic fragments from photooxidation of disposable plastic boxes. Sci Total Environ 858. https://doi.org/10.1016/j.scitotenv.2022.160044.
[20] Almond, J., Sugumaar, P., Wenzel, M.N., Hill, G., Wallis, C., 2020. Determination of the carbonyl index of polyethylene and polypropylene using specified area under band methodology with ATR-FTIR spectroscopy. E-Polym 20, 369–381. https://doi.org/10.1515/epoly-2020-0041.
[21] E. Kuttainen, M. Walfridson, Automation of carbonyl index calculations for fast evaluation of microplastics degradation, 2022.
[22] Kitahara, K.I., Nakata, H., 2020. Plastic additives as tracers of microplastic sources in Japanese road dusts. Sci Total Environ 736. https://doi.org/10.1016/j.scitotenv.2020.139694.
[23] Yamahara, S., Kubota, R., Tun, T.Z., Nakata, H., 2024. Source traceability of microplastics in road dust using organic/inorganic plastic additives as chemical indicators. Sci Total Environ 932. https://doi.org/10.1016/j.scitotenv.2024.172808.
[24] Schmidt, K., Atkinson, A., Stübing, D., McClelland, J.W., Montoya, J.P., Voss, M., 2003. Trophic relationships among Southern Ocean copepods and krill: Some uses and limitations of a stable isotope approach. Limnol Oceanogr 48, 277–289. https://doi.org/10.4319/lo.2003.48.1.0277.
[25] Annable, W.K., Frape, S.K., Shouakar-Stash, O., Shanoff, T., Drimmie, R.J., Harvey, F.E., 2007. 37Cl, 15N, 13C isotopic analysis of common agro-chemicals for identifying non-point source agricultural contaminants. Appl Geochem 22, 1530–1536. https://doi.org/10.1016/j.apgeochem.2007.03.049.
[26] Rumolo, P., Barra, M., Gherardi, S., Marsella, E., Sprovieri, M., 2011. Stable isotopes and C/N ratios in marine sediments as a tool for discriminating anthropogenic impact. J Environ Monit 13, 3399–3408. https://doi.org/10.1039/c1em10568j.
[27] Elsner, M., Jochmann, M.A., Hofstetter, T.B., Hunkeler, D., Bernstein, A., Schmidt, T.C., Schimmelmann, A., 2012. Current challenges in compound-specific stable isotope analysis of environmental organic contaminants. Anal Bioanal Chem 403, 2471–2491. https://doi.org/10.1007/s00216-011-5683-y.
[28] Hunkeler, D., Laier, T., Breider, F., Jacobsen, O.S., 2012. Demonstrating a natural origin of chloroform in groundwater using stable carbon isotopes. Environ Sci Technol 46, 6096–6101. https://doi.org/10.1021/es204585d.
[29] Alberti, M., Fürsich, F.T., Abdelhady, A.A., Andersen, N., 2017. Middle to Late Jurassic equatorial seawater temperatures and latitudinal temperature gradients based on stable isotopes of brachiopods and oysters from Gebel Maghara, Egypt. Palaeogeogr Palaeoclimatol Palaeoecol 468, 301–313. https://doi.org/10.1016/j.palaeo.2016.11.052.
[30] Giebel, B.M., Cime, S., Rodgers, L., Li, T.De, Zhang, S., Wang, T., 2022. Short-term exposure to soils and sludge induce changes to plastic morphology and 13C stable isotopic composition. Sci Total Environ 821. https://doi.org/10.1016/j.scitotenv.2022.153375.
[31] González-Pérez, J.A., Jiménez-Morillo, N.T., de la Rosa, J.M., Almendros, G., González-Vila, F.J., 2015. Pyrolysis-gas chromatography-isotope ratio mass spectrometry of polyethylene. J Chromatogr A 1388, 236–243. https://doi.org/10.1016/j.chroma.2015.02.039.
[32] Berto, D., Rampazzo, F., Gion, C., Noventa, S., Ronchi, F., Traldi, U., Giorgi, G., Cicero, A.M., Giovanardi, O., 2017. Preliminary study to characterize plastic polymers using elemental analyser/isotope ratio mass spectrometry (EA/IRMS). Chemosphere 176, 47–56. https://doi.org/10.1016/j.chemosphere.2017.02.090.
[33] Birch, Q.T., Potter, P.M., Pinto, P.X., Dionysiou, D.D., Al-Abed, S.R., 2021. Isotope ratio mass spectrometry and spectroscopic techniques for microplastics characterization. Talanta 224. https://doi.org/10.1016/j.talanta.2020.121743.
[34] Goudriaan, M., Morales, V.H., van der Meer, M.T.J., Mets, A., Ndhlovu, R.T., van Heerwaarden, J., Simon, S., Heuer, V.B., Hinrichs, K.U., Niemann, H., 2023.

A stable isotope assay with 13C-labeled polyethylene to investigate plastic mineralization mediated by Rhodococcus ruber. Mar Pollut Bull 186. https://doi.org/10.1016/j.marpolbul.2022.114369.

[35] Vidal-Abad, A., Casal, M.A., Rey-Aguiño, J.M., Pichel-González, A., Solana-Muñoz, A., Poza-Nogueiras, V., Varela, Z., Galbán-Malagón, C., Ouro, P., Fernández-Sanlés, A., 2024. Case report of plastic nurdles pollution in Galicia (NW Atlantic) following the Toconao's spill in December 2023: The VIEIRA Collaborative. Mar Pollut Bull 203. https://doi.org/10.1016/j.marpolbul.2024.116442.

[36] Marturano, V., Cerruti, P., Ambrogi, V., 2019. Polymer additives. Phys Sci Rev 2. https://doi.org/10.1515/psr-2016-0130.

[37] Schwab, S.T., Baur, M., Nelson, T.F., Mecking, S., 2024. Synthesis and deconstruction of polyethylene-type materials. Chem Rev 124, 2327–2351. https://doi.org/10.1021/acs.chemrev.3c00587.

[38] Pack, A., Höweling, A., Hezel, D.C., Stefanak, M.T., Beck, A.K., Peters, S.T.M., Sengupta, S., Herwartz, D., Folco, L., 2017. Tracing the oxygen isotope composition of the upper Earth's atmosphere using cosmic spherules. Nat Commun 8. https://doi.org/10.1038/ncomms15702.

[39] Kroopnick, P., Craig, H., 1972. Atmospheric oxygen: isotopic composition and solubility fractionation. Science 175 (1979), 54–55. https://doi.org/10.1126/science.175.4017.54.

[40] Mader, M., Schmidt, C., van Geldern, R., Barth, J.A., 2017. Dissolved oxygen in water and its stable isotope effects: a review. Chem Geol 473, 10–21. https://doi.org/10.1016/j.chemgeo.2017.10.003.